Constraints Imposed by the Membrane Selectively Guide the Alternating Access Dynamics of the Glutamate Transporter Glt_{Ph}

Timothy R. Lezon and Ivet Bahar

Department of Computational and Systems Biology, University of Pittsburgh, Pittsburgh, Pennsylvania

Supporting Material

Cumulative overlap. The deformation vector **d** between structures *a* and *b* (referring to the IF and OF conformations in the present case) is defined as

$$\mathbf{d} = \left[\left(x_1^b - x_1^a \right) \quad \left(y_1^b - y_1^a \right) \quad \left(z_1^b - z_1^a \right) \quad \ldots \left(z_N^b - z_N^a \right) \right]^T , \tag{S1}$$

where the coordinates are taken from the optimally aligned structures (ref. 47). Given the ordered set of 3*N*-6 normalized eigenvectors $\{\boldsymbol{v}\} = \{\boldsymbol{v}_i, \ldots, \boldsymbol{v}_{3N-6}\}$ of **H** that define the entire space of internal motions, the cumulative overlap of **d** with the first *m* vectors of {**v**} is

$$O^m(\mathbf{d}) = \frac{1}{|\mathbf{d}|} \left[\sum_{k=1}^{m} (\mathbf{d} \cdot \mathbf{v}_k)^2 \right]^{1/2} . \tag{S2}$$

The value of $O^m(\mathbf{d})$ increases monotonically with *m* from zero at *m*=0 to one at *m*=3*N*-6.

Net radial motion. To measure the net outward radial motion induced by the kth mode $\boldsymbol{v}_k$, we define the net radial component of the 3*N* dimensional unit vector $\boldsymbol{v}_k = [\boldsymbol{v}_k^{(1)} \ \boldsymbol{v}_k^{(2)} \ \boldsymbol{v}_k^{(3)} \ \ldots \boldsymbol{v}_k^{(N)}]^T$ as

$$f_\rho(\boldsymbol{v}_k) = \left| \frac{1}{\sqrt{N}} \sum_{i=1}^{N} \boldsymbol{v}_k^{(i)} \cdot \hat{\boldsymbol{\rho}}_i \right| , \tag{S3}$$

where $\hat{\boldsymbol{\rho}}_i$ is the unit vector along the radial component of residue *i* position vector, expressed in cylindrical coordinates (with the origin at the center of mass and the *z*-axis along the axial direction, perpendicular to the membrane, pointing outward to the EC region).

Residue-residue cosines. The vector $\mathbf{v}_i^k = (x_i^k, y_i^k, z_i^k)^T$ describes the motion induced in residue *i* by mode *k*, $\mathbf{v}^k = (x_1^k, y_1^k, z_1^k, \ldots, x_N^k, y_N^k, z_N^k)^T$. We define the cosine between the directions of motion of residues *i* and *j* in mode *k* as

$$\cos_{ij}^k = \frac{\mathbf{v}_i^k \cdot \mathbf{v}_j^k}{\left| \mathbf{v}_i^k \right| \left| \mathbf{v}_j^k \right|} . \tag{S4}$$

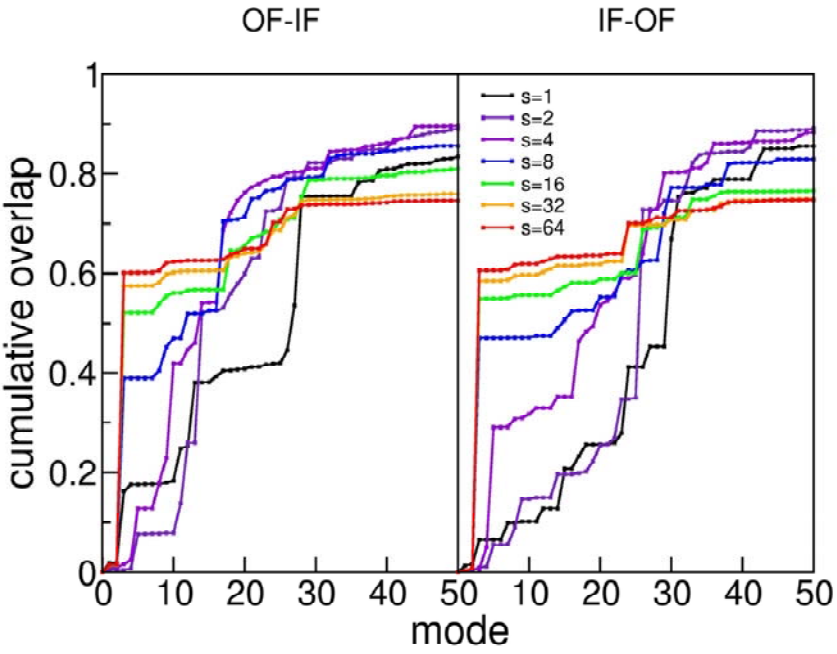

Figure S1: The value of the *im*ANM membrane scaling factor, *s*, determines the relative contributions of the modes to the cumulative overlap. As *s* increases, so does the contribution of the slowest non-degenerate mode. We have empirically determined that a scaling factor of *s*=16 permits a significant contribution from this mode while not entirely distorting the effects of the higher modes.

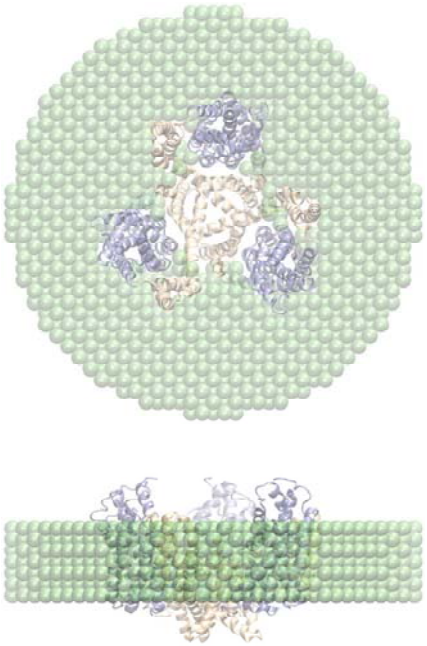

Figure S2: The *ex*ANM model consists of the protein and a fragment of the membrane modeled with an ENM.

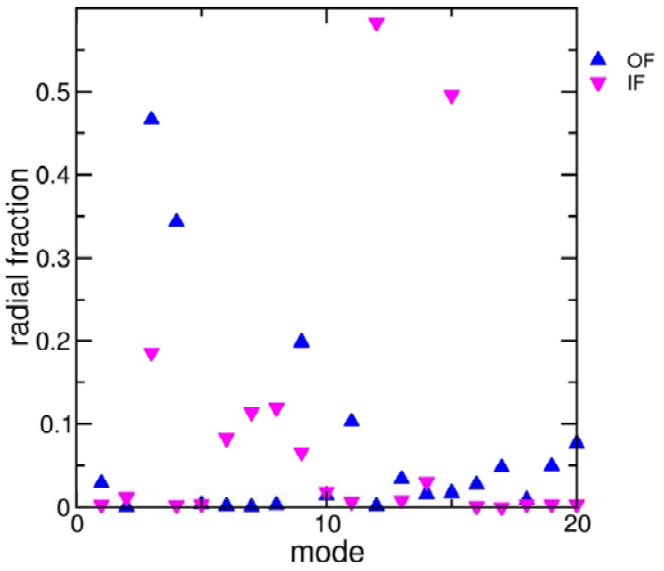

Figure S3: The slowest ANM modes of Glt_{Ph} have large radial components. The net radial fraction (see Methods in main text and Eq. S3) is plotted for the first 20 ANM modes of the OF (blue) and IF (magenta) conformations. The third and fourth modes of the OF conformation have large radial components, whereas the equivalent modes of the IF conformation are radially less intense. The *ex*ANM attenuates the radial motion of the OF conformation, but leaves the motion of the IF conformation largely unchanged.

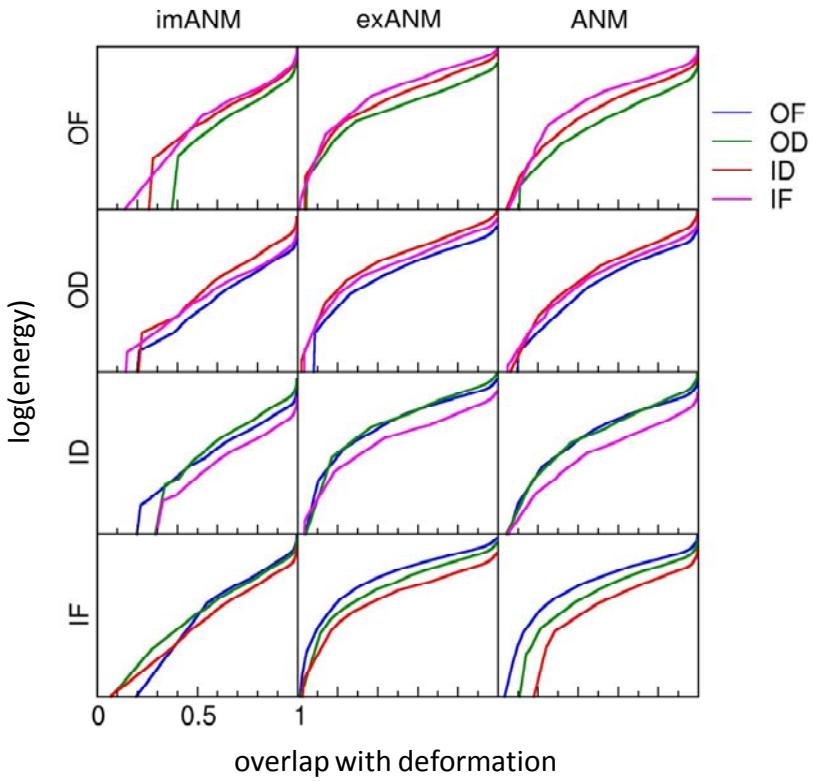

Figure S4: Transitions to intermediate states (OD and ID) are energetically favored. Plots show the energy required for deformations from the initial states shown at left to the final states indicated by curve color. In the top row, it is clear that transitions from the OF conformation to the OD (green) conformation carry lower in energy than deformations to either the ID (red) or IF (magenta) conformations. The second row shows that the lowest energy transition starting from the OD conformation is to the OF (blue) conformation, indicating that the favored motion is of a single subunit between the outward- and inward-facing conformations. A similar motion is observed between the IF and ID structures (bottom two rows). These results hold for all three ENMs investigated.

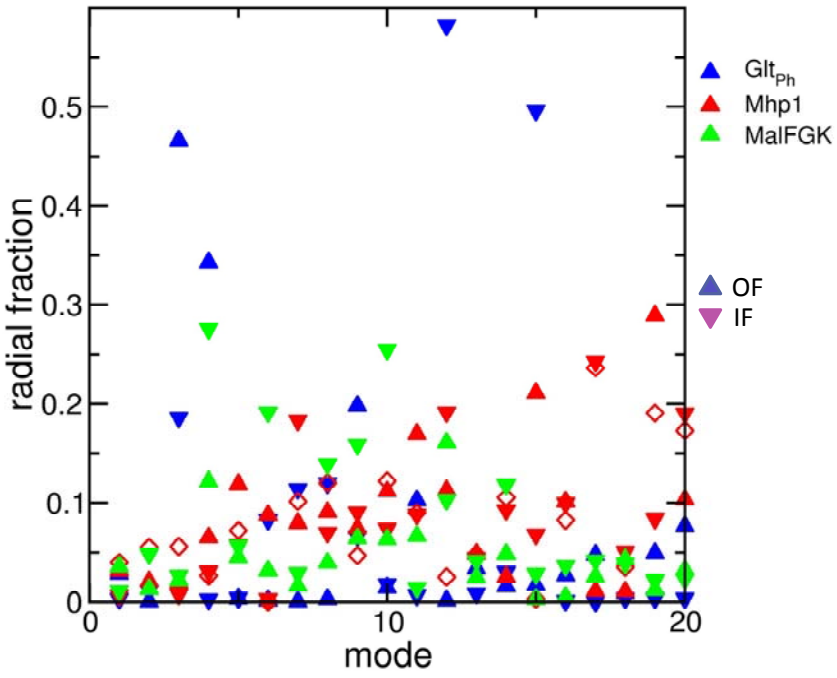

Figure S5: Same as Figure S3, for illustrating the distinctive character of Glt_{Ph} slowest modes compared to those of two other transporters, Mhp1 and MalFGK, structurally resolved in IF and OF forms. Glt_{Ph} (blue) shows the largest radial components among the three transporters. Note that the relatively large radial component in mode 4 (IF structure) of MalFGK mainly pertains to the large intracellular portion of the transporter, such that the radial constraints exerted by the lipid bilayer are not as significant as those affecting Glt_{Ph} dynamics, which is mostly embedded in the membrane.